ADVANCED OPTICAL MATERIALS
www.advopticalmat.de

Light-Responsive (Supra)Molecular Architectures: Recent Advances

Massimo Baroncini, Jessica Groppi, Stefano Corra, Serena Silvi, and Alberto Credi**

The development and investigation of (supra)molecular-based architectures characterized by light-activated functionalities is a highly relevant topic of chemical research. The interest on photo-controlled systems arises not only from their potential applications in different fields of technology but also from their scientific significance related to the understanding of light–matter interactions at the nanoscale. Indeed, light is a peculiar and unique tool as it can be conveniently applied to supply the energy required to affect and operate a system and, at the same time, to probe its state and investigate its transformations. Some basic aspects of light-induced processes in (supra) molecular architectures are discussed here in the frame of their use to implement novel functionalities in nanostructured systems and materials. In this perspective, a few recent examples from our own work will be illustrated which are meant to provide an overview of the current directions in this highly cross-disciplinary field of research.

1. Introduction: Light to Operate and Control Molecular and Supramolecular Architectures

The interaction between light and matter is fundamental for some of the most relevant natural and artificial processes. Indeed, light radiation is utilized both in natural and artificial systems as an energy source and as a tool to transfer and manipulate information. Nature exploits light as the main power source in natural photosynthesis, while it harnesses the information content of light radiation in the processes related to vision.[1] Also modern technology, by means of fundamental processes analogous to the natural ones, despite the use of much less sophisticated architectures, has achieved many of its life-changing revolutions by exploiting the interaction between light and matter in artificial systems to transform energy and manipulate information.[2] The type and utility of the functions attained in artificial systems depend on the degree of complexity and organization of the chemical entities composing the systems themselves that collect and process the photons. Supramolecular chemistry, a branch of chemistry that deals with the "organized entities of higher complexity that result from the association of two or more chemical species held together by intermolecular forces"[3] is intimately related to advancements in the realization of artificial systems able to display sophisticated functionalities. The monumental progresses of synthetic chemistry during the last century allow today's chemists to synthesize even highly complex molecules almost at will, enabling the design and realization of an endless variety of molecular architectures with the most disparate structures.[4] Similarly, the vast amount of research in the last three decades on the supramolecular organization of matter allow researchers to rationally develop molecular moieties able to self-assemble, in opportune conditions, into supramolecular architectures of high complexity.[5] It is important to note that (supra)molecular architectures can also be realized where the different molecular components are held together not by weak intermolecular forces but by strong and directional dative and covalent bonds (as in covalent and metal organic frameworks, dendrimers, and coordination polymers) or even by mechanical interlocking such as in mechanically interlocked molecules (MIMs, exemplified by rotaxanes and catenanes).[6] According to the most stringent definition of supramolecule, such systems do not belong to the supramolecular realm; nevertheless, it is important to point out that species that are not supramolecules when analyzed from a strict bond-type perspective, in fact, behave as supramolecules if scrutinized from a physico-chemical point of view and the related emerging functions are considered. It has been proposed to modify the definition of a supramolecular system by overcoming a stringent consideration of the nature of the bond holding together the different components, toward a definition based on the identification of discrete "functional moieties," in analogy to the definition of "functional groups" adopted in organic chemistry.[7] Whenever in a large molecule, or in an assembly of molecules, different functions can be assigned to a specific grouping of atoms, that system can be considered supramolecular, that is, made by a discrete number of functional moieties (i.e., molecules or part of them) held

Dr. M. Baroncini, Dr. J. Groppi, Dr. S. Corra, Prof. A. Credi
CLAN-Center for Light Activated Nanostructures
Dipartimento di Scienze e Tecnologie Agro-Alimentari
Università di Bologna
via Gobetti 101, 40129 Bologna, Italy
E-mail: massimo.baroncini@unibo.it; alberto.credi@unibo.it
Dr. M. Baroncini, Dr. J. Groppi, Dr. S. Corra, Prof. A. Credi
Istituto ISOF-CNR
via Gobetti 101, 40129 Bologna, Italy
Dr. S. Silvi
Dipartimento di Chimica "G. Ciamician"
Università di Bologna
Via Selmi 2, 40126 Bologna, Italy
The ORCID identification number(s) for the author(s) of this article can be found under https://doi.org/10.1002/adom.201900392.

DOI: 10.1002/adom.201900392

together by different forces, from weak intermolecular electrostatic interactions to strong covalent bonds.

With the development of supramolecular chemistry, it was proposed that the concept of a macroscopic device could be applied to the molecular level.[8] In brief, a molecular device can be defined as a supramolecule (using the wider definition detailed above) assembled from a discrete number of components designed to perform a function under appropriate external stimulation. The most fascinating types of molecular devices are molecular machines and motors: systems that once were powered by an energy source can achieve controlled mechanical movements of their components.[9] The fundamental scientific value of these ideas and their huge—albeit, at present, unexpressed—potential for applications led to the award of the Nobel Prize in Chemistry in 2016 to Jean-Pierre Sauvage, Fraser Stoddart, and Ben Feringa "for the design and synthesis of molecular machines."[10]

Besides recognition of the significance of molecular devices by the scientific community, the realization (thanks to the progresses of molecular biology) that the foundation of life is based on a formidable array of natural nanomachines is responsible for much of the stimulus to develop artificial analogues.[11] Indeed, the supramolecular architectures of the biological world are the most evident proof of the feasibility and utility of nanotechnology and provide a strong incentive to attempting the realization of artificial molecular devices. However, the impressive complexity of the nanoarchitectures employed by nature to achieve its aims makes mere replication a prohibitive task. Thus, scientists have developed and synthesized simpler architectures, with no intention to replicate the complex designs of the biological structures but only to imitate their functions.[12]

To enable the transition of artificial molecular devices from simple laboratory curiosities to key components of novel disruptive technologies, besides comprehending the fundamental principles and the processes by which molecular devices operate, a most daunting challenge has to be confronted: interfacing nanometer-sized molecular objects with the macroscopic world, principally in relation to energy supply and information exchange. Indeed, molecular devices, similarly to their macroscopic analogues, require an energy source to operate and signaling pathways to communicate with the environment.[13] Light is an ideal tool to fulfill both these requirements: light is able to "read" the state of a system, enabling the monitoring of its operations, because the photophysical properties of a system are usually strongly affected by the interactions between its components. On the other hand, photons can induce reactions ("write") that, by means of reversible structural and/or electronic modifications, can switch the chemical and physical properties of a system, thus allowing the realization of light-powered functionalities.[14] Indeed, the study of systems in which chemical, physical, and other relevant properties can be modulated as a result of a light-induced transformation is a very active area of research.[15] Photoswitchable molecular systems have been designed and investigated both as individual species in solution and, more recently, in supramolecular assemblies at interfaces, surfaces, and in the solid state.[16] It is therefore not surprising that the growth of the field of stimuli-responsive materials is strictly related to the progress of research on photoreactive molecular moieties.[17]

Massimo Baroncini is currently assistant professor of chemistry at the University of Bologna, Italy, and researcher at the Center for Light Activated Nanostructures (CLAN). He has coauthored over 50 scientific publications and one monograph. His main research activity deals with the synthesis and investigation of supramolecular systems with tailored physico-chemical functionalities.

Alberto Credi is professor of chemistry at the University of Bologna, Italy, and director of the Center for Light Activated Nanostructures (CLAN), a University–National Research Council joint laboratory for research in photochemistry, supramolecular chemistry, materials science, and nanoscience. He has coauthored four books and over 280 scientific publications, and he is the PI of an ERC Advanced Grant for the development of light-driven molecular motors.

The objective of this perspective is to present and describe some recent molecular and supramolecular architectures based on one of the most studied and exploited light-activated molecular switches, azobenzene.[18] Its application as a tool to operate ("write") and communicate ("read") with molecular and supramolecular architectures will be illustrated through some selected examples taken from our recent work, which are also intended to exemplify the state of current research in this field and potential applications, limitations, and future directions.

2. Azobenzene

2.1. Probably the Best Light Actuator that Chemistry has to Offer

Upon absorption of light of appropriate wavelength, typically in the range between 200 and 1000 nm, a molecule can be promoted to an electronically excited state, which is a transient metastable species with radically different physico-chemical properties compared to the ground state. Molecules in the excited state undergo rapid deactivation by different competitive processes: radiative decay that results in different forms of luminescence, non-radiative decay, and photoreactions. One of the most widely investigated and exploited class of unimolecular light-induced reactions is photoisomerization.[19]

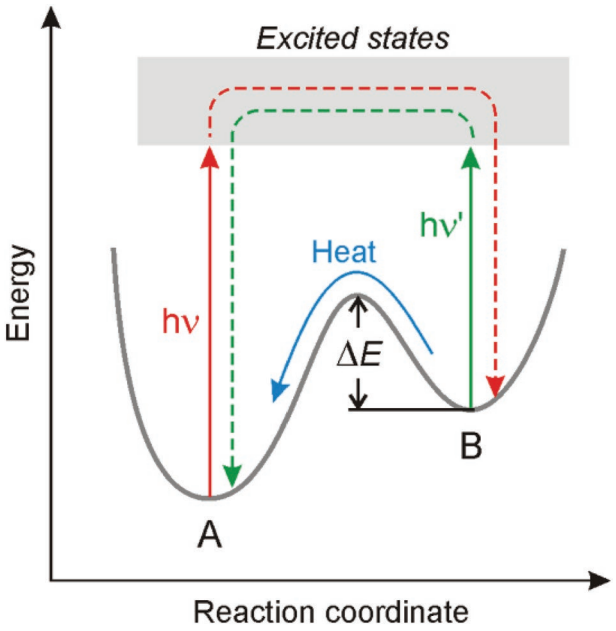

Figure 1. Simplified energy profile for the interconversion between the two isomers of a photochromic system.

A photoisomerization reaction is characterized by the transformation of a compound from one isomeric form to another caused by light irradiation. In most instances, the interconvertible forms are configurational *E*-*Z* stereoisomers or open- and closed-ring isomers. Azobenzene, stilbene, flavylium, and hydrazone are prototypical classes of compounds undergoing *E*→*Z* configurational photoinduced isomerization, while diarylethenes, spiropyrans, fulgides, and dihydroazulenes provide examples of ring closing and opening photoreactions.

Species of this kind are often named photochromic compounds, or photochromes, because the interconvertible forms usually exhibit different absorption spectra (i.e., color). More recently, the term "molecular photoswitches" has come into use to refer to photochromic molecular entities.[20] In general terms, light excitation in a photochromic compound (hν) causes the conversion from a stable isomer A to a higher energy isomer B (**Figure 1**). The latter is expected to spontaneously reconvert to the former through a thermal back reaction by overcoming an energy barrier (ΔE in Figure 1). While the photoinduced A→B transformation is usually very fast, the thermal B→A reaction can be fast or slow, depending on the system. In some cases the photoproduct B is kinetically inert and the process can only be reverted by using a second optical stimulus (hν'). Photochromic systems can thus be divided in two classes: thermally reversible (T-type) photochromes, in which the photogenerated isomer B can revert thermally to the initial form, and photochemically reversible (P-type) photochromes, in which the back reaction is exclusively promoted by light irradiation. Azobenzenes and spiropyrans belong to the T-type class, while most diarylethenes are examples of the P-type class.

The importance of photochromic compounds originates from the consideration that the most straightforward and, for that reason, one of the most explored strategies to engineer photoactive architectures entails the chemical functionalization of their molecular building blocks with photochromic moieties, able to sustain a reversible photochemical process.[16] In this regard, the light-induced E→Z switching of the −N=N− double bond in azobenzene, one of the oldest and most studied photochromic moieties, represents a prototypical example.[20]

Azobenzene was first described by E. Mitscherlich in 1834[21] and the first large-scale synthetic procedure developed by Alfred Nobel dates back to 1856.[22] In the later years, the chemistry of azobenzene and its derivatives was intensely investigated, owing to its fundamental importance in the dyes and pigments industry. Only in 1910, Gortner and co-workers, as a consequence of the growing interest and understanding concerning the stereochemistry of organic compounds, published a first pioneering work proposing the possible existence of *syn* (*Z*) and *anti* (*E*) stereoisomeric forms of azobenzene.[23] The *Z* stereoisomer of azobenzene and the *E*→*Z* photoisomerization reaction were eventually discovered only in 1937 by G. S. Hartley, who was able to prove the formation of *Z* azobenzene by careful solvent extraction after light irradiation.[24] Since then, and in particular during the past 30 years, azobenzene has grown in interest and popularity in the scientific community, and a myriad of experimental and computational studies involving azobenzene photoisomerization have been published.[25] Beyond the fundamental research on the chemical and physical properties, the most widespread present application of azobenzene derivatives in nanotechnology is the design and realization of materials and nano-devices able to carry out movements and functions triggered by light stimuli.

Azobenzene photoisomerization is an ideal process to obtain light-driven functionalities in suitably designed molecular and supramolecular systems in order to develop, for example, photoactive drugs, devices, and materials. Present and forthcoming applications of research on azobenzene-based materials include holography,[26] photolithography,[27] optoelectronic devices, magnetic memories, control of chemical reactivity and biochemical functions,[28] responsive surfaces and materials,[29] and energy conversion.[30] The unique properties of azobenzene and its derivatives, together with their synthetic accessibility and versatility and the possibility of tuning their spectroscopic and photochemical behavior by chemical functionalization, are the main reasons why this class of compounds is widely regarded as the best photochromic moiety that chemistry has to offer.[31]

In the following sections a brief description of the basic physico-chemical properties of azobenzene will be given, and its exploitation for photo-inducing and controlling functional transformations in supramolecular systems in solution and in the solid state will be illustrated with some recent examples investigated in our laboratory.

2.2. Relevant Chemical and Photochemical Properties of Azobenzene and Its Derivatives

The most important feature of azobenzene, concerning its applicability to develop light-responsive architectures, is the marked difference in the structure and properties of the two stereoisomeric forms (**Figure 2**a). Azobenzene in the *E* configuration is ≈42 kJ mol^{-1} more stable than that in the *Z* form; for this reason, at equilibrium in the dark, azobenzene

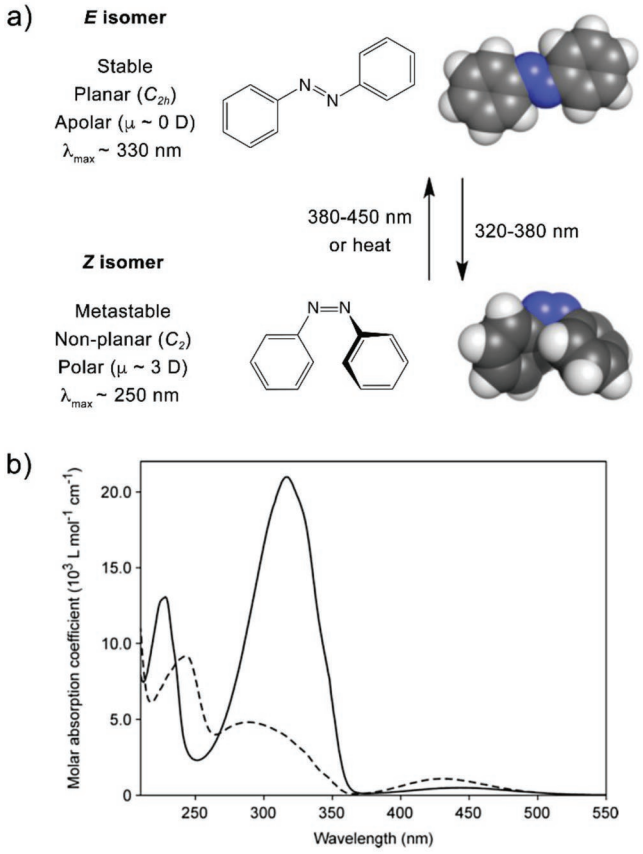

Figure 2. a) The *E* and *Z* isomers of azobenzene and their photo- and thermally induced interconversion. b) UV–visible absorption spectra of *E*- (full line) and *Z*-azobenzene (dashed line) in acetonitrile at room temperature.

occurs almost exclusively as its *E* stereoisomer. X-ray data show that the *E* form is practically planar with C_{2h} symmetry, while the *Z* form is characterized by a non-planar configuration with a dihedral angle of ≈45° along the CNNC bonds and is characterized by C_2 symmetry. The large geometrical change accompanying *E*→*Z* isomerization is also revealed by the substantial variation in the distance between the carbon atoms in the *para* positions of the phenyl rings that decreases from 10 to 4 Å on going from the *E* to *Z* configuration.[18] These significant structural differences are reflected by a large differentiation in the chemical and physical properties of the two stereoisomers. Among those properties, the one that led to the discovery of photochromism in azo compounds is solubility. Indeed, while *E*-azobenzene is a non-polar molecule highly soluble in apolar organic solvents, the *Z* stereoisomer has a dipole moment of ≈3 Debye and can be dissolved in highly polar solvents such as water.[32] The two stereoisomeric forms of azobenzene possess distinct, albeit largely overlapping, absorption spectra in solution. In acetonitrile, for example (Figure 2b), the *E* isomer shows a broad and intense band (ε = 21000 M^{-1} cm^{-1}) at 316 nm, assigned to a $\pi\pi^*$ electronic transition, and a weaker band (ε = 550 M^{-1} cm^{-1}) with an absorption maximum at 445 nm, assigned to a $n\pi^*$ transition. The *Z* form also has two characteristic $\pi\pi^*$ and $n\pi^*$ bands with absorption maxima at 279 (ε = 4300 M^{-1} cm^{-1}) and 428 nm (1200 M^{-1} cm^{-1}), respectively (Figure 2b).[33]

The presence of substituents on the aromatic rings can induce radical changes on the absorption spectra and photochemical properties of azobenzene. Functionalized azobenzenes have been categorized by Rau, according to their different spectroscopic characteristics, into three classes based on the relative energies of $\pi\pi^*$ and $n\pi^*$ transitions (**Figure 3**a).[34]

The first class comprises plain azobenzene and azobenzenes whose phenyl rings bear alkyl, aryl, halide, carbonyl, amide, nitrile, ester, and carboxylic acid substituents. All these species show the typical features of unsubstituted azobenzene, namely, two distinct $\pi\pi^*$ and $n\pi^*$ absorption bands and a thermal reaction from the photogenerated *Z* form to the thermodynamically stable *E* form occurring in solution at room temperature on a timescale from hours to days.

Aminoazobenzene is the prototypical compound representative of the second class of azobenzene derivatives according to Rau's classification (Figure 3a). Azobenzenes functionalized with amino, hydroxyl, and alkoxy substituents are characterized spectroscopically by a shift of the $\pi\pi^*$ absorption band to longer wavelengths, such that it becomes partially overlapped with the $n\pi^*$ band. Aminoazobenzenes exhibit significantly faster thermal isomerization rates compared to azobenzene, with a half-life of the *Z* forms in the range of seconds to minutes.

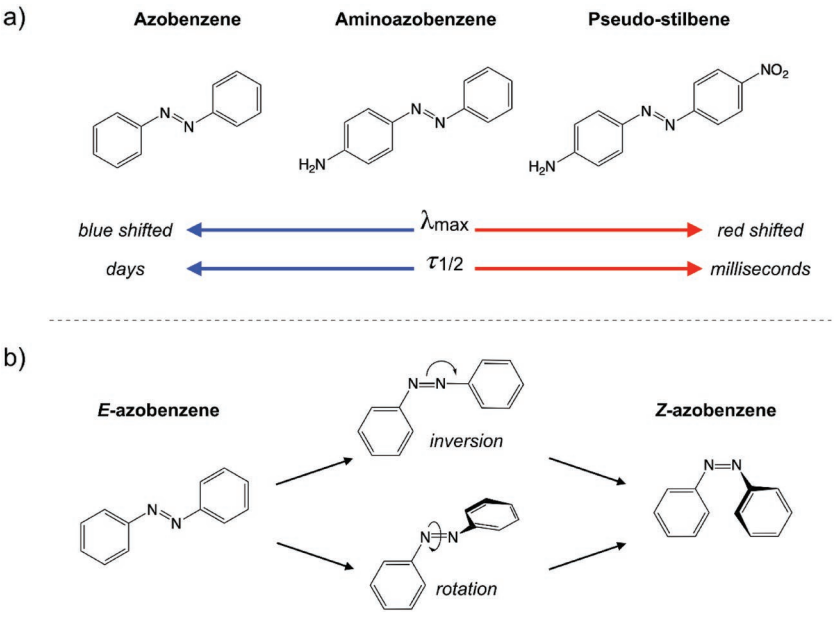

Figure 3. a) The three classes of azobenzene according to Rau's classification and the corresponding variation of the absorption maximum of the *E*-form (λ_{max}) and the half-life at room temperature of the *Z*-form ($\tau_{1/2}$). b) The rotation and inversion mechanisms for the *E*→*Z* isomerization of azobenzene.

The third class of azobenzene derivatives is represented by the pseudo-stilbenes (Figure 3a). The exemplary compounds are the protonated form of azobenzene and push-pull azobenzenes (i.e., azobenzenes substituted with an electron donor group on one phenyl ring and an electron acceptor group on the other). This class is characterized spectroscopically by a complete overlap of the $\pi\pi^*$ and $n\pi^*$ absorption bands and an extremely fast thermal back conversion, with a half-life of the *Z* stereoisomer ranging from milliseconds to seconds.

This short description of the main classes of azobenzene derivatives should make evident that appropriate engineering of the chemical structure enables a straightforward and predictable tuning of the photophysical and chemical parameters of azobenzene-based species to match the optical and kinetic requirements needed for a specific application. However, regardless of the well-understood structure-property relationships in azobenzene derivatives, it is still rather difficult to engineer compounds able to absorb in the red and near-infrared spectral region, a key wavelength range for biomedical and security applications.[31]

Despite the large amount of investigations, dating back to the first time the *Z* isomer was isolated and identified by Hartley, the detailed mechanism of isomerization of azobenzene and its derivatives has been the subject of much controversy.[35] Indeed, this problem has challenged experimentalists[36] and theoreticians[37] for many years and remains a debated issue even today. The isomerization mode (thermal vs light induced), irradiation wavelength, solvent properties, substitution pattern, temperature, and pressure markedly influence the isomerization mechanism and quantum yield of the photoprocess. In general, two basic pathways are considered: the in-plane increase of the Ph−N=N angle (inversion mechanism), and the torsion of the molecule around the N=N axis (rotation mechanism) (Figure 3b). Despite a lack of agreement on the details of the mechanism for many azobenzene derivatives, by far the most important aspect of azobenzene photochromism is that the light-induced isomerization reaction is an exceptionally clean and fatigue-resistant reaction taking place with generally high quantum yields and minimal decomposition.[38] For practical applications, however, the possibility to manipulate the photoisomerization quantum yield and the rate of thermal back isomerization is more important than a detailed knowledge of the mechanistic aspects of the isomerization reaction. One possible drawback to consider in applications exploiting azobenzene photochromism is that since both *E* and *Z* stereoisomers are photoreactive and exhibit absorption spectral overlap (Figure 2b), irradiation of either isomer produces a photostationary state containing a mixture of *E* and *Z* isomers. The stereoisomeric composition of the photostationary state depends on the molar absorption coefficients and photoisomerization quantum yields of the two forms at the specific irradiation wavelength.[39] Controlling the absorption characteristics of azobenzene derivatives through chemical functionalization is thus a key prerequisite for applications that require a clean and quantitative switching between the two isomeric forms.

Nowadays, photoactive molecular and supramolecular systems that base their function on the photoisomerization of azobenzene moieties have reached a high level of sophistication, as exemplified by the systems described in the next sections.

3. Photoactive Molecular and Supramolecular Architectures

3.1. Photoswitchable Molecular Materials Based on Azobenzene Tetramers

In most instances, the reactivity of photochromic compounds has been investigated in dilute solution, or, in fewer cases, in soft matrices such as gels and flexible polymers wherein the photochrome is employed as a dopant. In recent years, the interest in photoisomerization reactions occurring in the crystalline solid state has enormously grown due to the various applications that novel tailor-made crystalline materials with light switchable properties can have in science and technology.[16] Diarylethenes represent one of the few classes of photochromic compounds able to undergo highly efficient and reversible single-crystal-to-single-crystal photoisomerization.[40] This almost unique characteristic has been exploited to obtain interesting photomechanical effects in solid crystalline materials.[41] Oppositely, the $E \rightarrow Z$ photoisomerization of azobenzene and of its derivatives does not occur in the crystalline state where the close packing of the molecular units obstructs the large steric volume changes associated with photoisomerization.[27] Indeed, the $E \rightarrow Z$ photoisomerization of azobenzene in the solid state is documented only in soft matrices such as polymers, gels, and liquid crystals and in porous materials with an ample void volume such as metal- and covalent organic frameworks.[42]

Recently, we developed a novel class of shape-persistent tetra(azobenzene)methane derivatives able to display efficient, reversible, and clean photoisomerization both in solution and in the solid crystalline state.[43] We investigated three different compounds (**1–3**, **Figure 4**a) consisting of four *E*-azobenzene units covalently linked to a central tetrahedral carbon atom, with different end groups in the *para* position of each azobenzene moiety (hydrogen for **1**, methyl for **2**, and *tert*-butyl for **3**). The rationale that guided us in developing a rigid arrangement of azobenzene photochromic units lays behind the consideration that a shape-persistent tetrahedral architecture of the molecule, combined with the stiffness of the azobenzene "arms" (Figure 4b), would hinder a tightly packed arrangement in the solid state.[44] The resulting crystal structure could therefore present enough available free volume, that is, porosity, combined with weak intermolecular interactions allowing photoisomerization of the azobenzene units in the solid crystalline state.[45] It is important to note that porous molecular crystals present different practical advantages when compared to other synthetic porous architectures such as metal–organic and covalent frameworks that can be summed up to easier synthetic procedures, facile structural diversification, and functional flexibility.[46]

All derivatives (**1–3**) were first characterized in dilute solution, where they show very similar spectroscopic and photochemical behavior; for this reason, only the properties of **3** (R = *t*-Bu) will be described as a representative case of this class of compounds. Irradiation with UV light (365 nm) of a

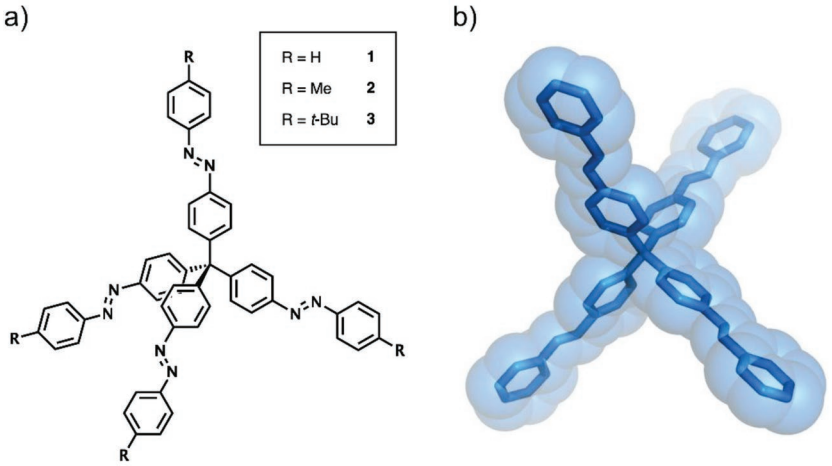

Figure 4. a) Structure formula of the shape-persistent azobenzene tetramers **1–3** in their all-*E* configuration. b) Molecular model of compound *EEEE*-**1**. Adapted with permission.[43] Copyright 2015, Nature Publishing Group.

solution of *EEEE*-**3** induces changes in the absorption spectrum consistent with the *E*→*Z* photoisomerization of the azo groups. However, it is important to evidence that throughout the irradiation isosbestic points are not fully conserved and the photoisomerization quantum yield decreases, a clear indication that the four azobenzene groups are not fully independent. The photostationary state reached upon exhaustive irradiation at 365 nm of **3** in deuterated benzene is composed of a mixture of five different stereoisomers (89% *ZZZZ*, 6% *EZZZ*, 3% *EEZZ*, <1% *EEEZ*, and <1% *EEEE*) with an overall *E*→*Z* conversion of all the azobenzene units of around 97%.

Crystallographic analysis of single crystals of the all-*E* isomers of **1–3** confirms that the rigid tetrahedral arrangement of the *E*-azobenzene moieties, and particularly in combination with bulky peripheral substituents as in the case of **3**, leads to a loose molecular packing in the solid state. Indeed, all the analyzed crystal structures are characterized by a significant amount of free volume in their crystal cell whose amount and shape strongly depend on the substitution pattern at the extremities of the azobenzene moieties. In particular, crystals of *EEEE*-**3** display 10.4% of free volume in the form of long channels spanning the whole crystal (**Figure 5**a). *EEEE*-**2** also exhibits a significant porosity (8.1% free volume) in the form of thinner channels compared to those of *EEEE*-**3** (Figure 5b), while in *EEEE*-**1**, the free volume (6.7%) is limited to isolated, non-communicating empty regions (Figure 5c). It is important to remark that all these molecular crystals exhibit porosity that result exclusively from the disposition of the individual molecules in the crystalline lattice. This type of porosity is defined as "intrinsic porosity," in opposition to "extrinsic porosity" that derives from cavities already present in the molecules that constitute the crystal itself and not from the packing geometry. Intrinsic porosity is particularly uncommon and of challenging design but a highly desirable characteristic since it is an emerging property that arises solely from the self-assembly of the individual molecules in the crystalline architecture.[46]

To elucidate the photoreactivity of **1–3** in the solid state, crystalline powders of the all-*E* isomers were drop-casted on quartz supports, irradiated at 365 nm, and then analyzed by X-ray powder diffraction, polarizing optical microscopy, UV–visible absorption spectroscopy, and ^{1}H NMR spectroscopy (after dissolution in deuterated benzene). NMR and UV–visible analysis of the irradiated samples prove that photoirradiation causes an efficient *E*→*Z* isomerization (32% *E*-to-*Z* conversion at the photostationary state for **3**), while X-ray diffraction and microscopic analysis of the films show that the photoisomerization reaction is concomitant with an amorphization of the material. The back *Z*→*E* transformation can be obtained in the thin solid films either upon visible irradiation or by heating. Interestingly, when the all-*E* form is regenerated by heating, the crystallinity of the sample is restored. All the materials show a high fatigue resistance. Alternated cycles of *E*→*Z* photoisomerization and *Z*→*E* heat-induced back transformations can be performed many times without appreciable degradation of the samples.

It is important to note that the melting point of *EEEE*-**3** is higher than 400 °C; thus, the liquid consistency of the amorphous material obtained by UV light at room temperature (**1** and **2** behave similarly) cannot be explained with a phase transition caused by the heating generated upon light irradiation. Actually, the photoinduced melting observed for azobenzene tetramers **1–3** is the result of a light-triggered isothermal phase transition due to the formation, at the photostationary state, of a mixture of stereoisomers characterized by a melting point lower than room temperature.[47] A similar behavior has

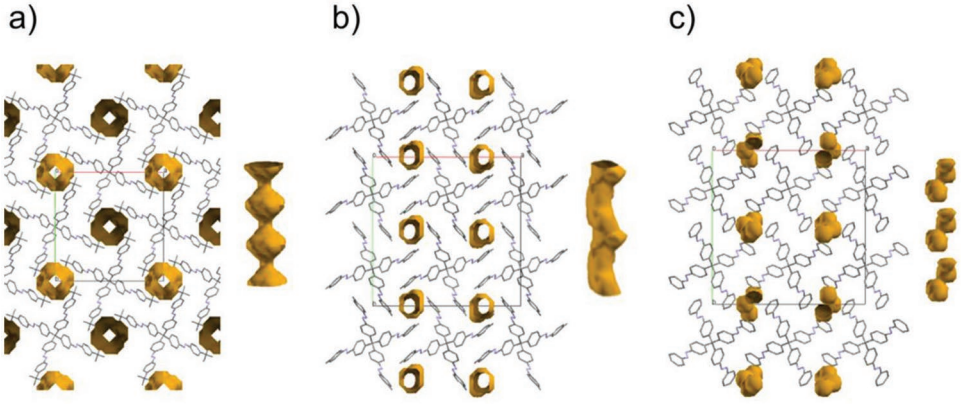

Figure 5. Stick representation of the crystal structure of the all-*E* isomers of **3** (a), **2** (b), and **1** (c) and space-filling view of the inner voids. The side view of the pores (channels for **3** and **2** and non-communicating voids for **1**) is shown in the right part of each panel. Hydrogen atoms are omitted for clarity. Adapted with permission.[43] Copyright 2015, Nature Publishing Group.

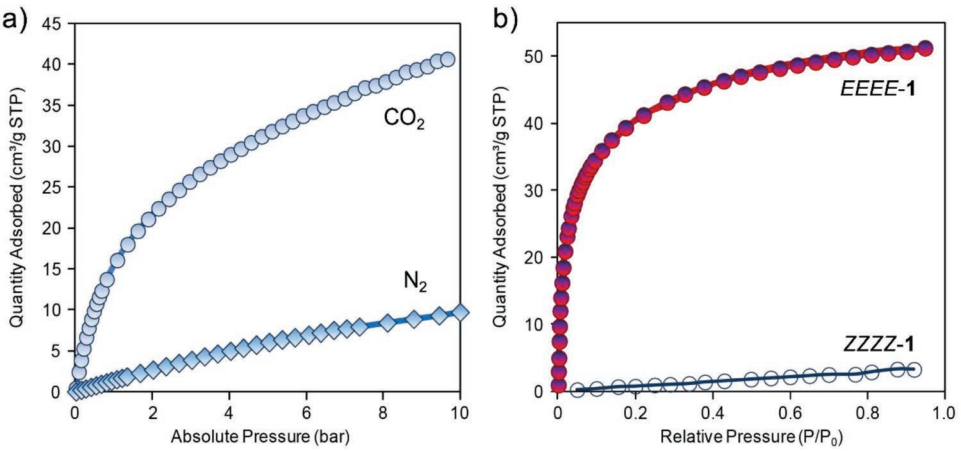

Figure 6. a) CO_2 (circles) and N_2 (diamonds) adsorption isotherms of *EEEE*-**1** at 273 K. b) CO_2 adsorption isotherms at 195 K of *EEEE*-**1** (filled circles) and *ZZZZ*-**1** (empty circles). Adapted with permission.[43] Copyright 2015, Nature Publishing Group.

been observed in a few other azobenzene-containing materials and is of interest for the development of photoresponsive coatings and adhesives.[48] Moreover, the changes in the aggregation state of the material and in the optical properties, in particular the switching of the birefringence of the film related to the loss of crystallinity caused by photoisomerization of the material, has implications for applications in information storage and cryptography.[49]

Detailed gas adsorption measurements were conducted to investigate the effect of photoisomerization on the porosity of these materials. While both **2** and **3** in their all-*E* forms exhibit N_2 and CO_2 Langmuir type-I adsorption isotherms due to the presence of channels extending through the whole crystal lattice (**Figure 6**a), *EEEE*-**1** shows negligible gas uptake as a consequence of the arrangement of the void volume in non-interconnected empty pores. Simple calculations confirm that two molecules of CO_2 are held inside each cavity of **2** and **3** at maximum CO_2 uptake (52 $cm^3\ g^{-1}$ for *EEEE*-**3** at 195 K and 1 bar); a figure consistent with the amount of empty space estimated from the analysis of the single-crystal structure, confirming the complete permeability of the porous crystal structure to gas molecules. Interestingly, **2** and **3** possess an appreciably large CO_2/N_2 selectivity (as high as 80 for *EEEE*-**2**), an unexpected characteristic that makes these materials relevant for gas separation applications such as the selective capture of CO_2 in flue gases (Figure 6a).

Contrary to the crystalline all-*E* forms, the CO_2 adsorption isotherms of the all-*Z* forms of **2** and **3** exhibit negligible gas uptake, indicating the absence of porosity (Figure 6b). The all-*Z* samples are quantitatively converted back to the porous all-*E* forms upon heating. Consequently, these materials can be switched between a crystalline porous and amorphous non-porous state by light irradiation and back by thermal $Z \rightarrow E$ isomerization of the azobenzene moieties. To date, this is the sole example in the literature of photoswitchable microporosity in a molecular crystal. Moreover, we recently proved that the shape-persistent tetrahedral disposition of the azobenzene groups in these materials appears to be a generalizable architecture to endow azobenzene-based compounds with the required combination of void space and weak interactions required to allow photoreactivity in the solid crystalline state, paving the way to a better understanding of solid-state photochemical reactions in azobenzene-based materials.

Another interesting possibility for these molecules, directly related to their rigid tetrapodal architecture, is their well-defined adsorption geometry on a solid surface. In fact, it can be anticipated that molecules such as **1–3** may behave as molecular-scale "caltrops" when landing on a surface, always leading to a configuration in which three azobenzene arms are in contact with the surface and the fourth one pointing away from it. Such an expectation is fully confirmed by scanning tunneling microscopy experiments performed on molecules of *EEEE*-**2** deposited on an atomically flat Ag(111) surface. It is well known that the photoreactivity of azobenzene is inhibited upon adsorption on a metallic surface due to the strong quenching effect on the excited state of the azo group by the metal electronic levels. In molecules of **2** adsorbed on an Ag(111) surface, however, the azobenzene arm pointing away from the surface, and thus detached from its influence, maintain its ability to isomerize in both directions under the action of either far field (light irradiation) or local (tip-induced current) stimuli. Remarkably, the ability of isolated molecules of **2** to diffuse on the metal surface depends on the isomeric configuration of the upward-pointing azobenzene unit, which in its turn can be switched by external stimulation. This study is significant because it describes a method to install photoactive molecules on surfaces while retaining their switching properties.[50] More generally, it highlights the importance of molecular design and of the possibilities that can arise from a precise control of the arrangement of functional moieties in multicomponent molecular architectures.[51]

3.2. Molecular Machines Controlled by Light

Molecular machines are supramolecular assemblies in which the components can be set in motion relative to one another in a controlled fashion in response to a chemical, optical, magnetic, or electrical stimulus, resulting in the potential ability to perform a specific task.[8] Research in this area is highly

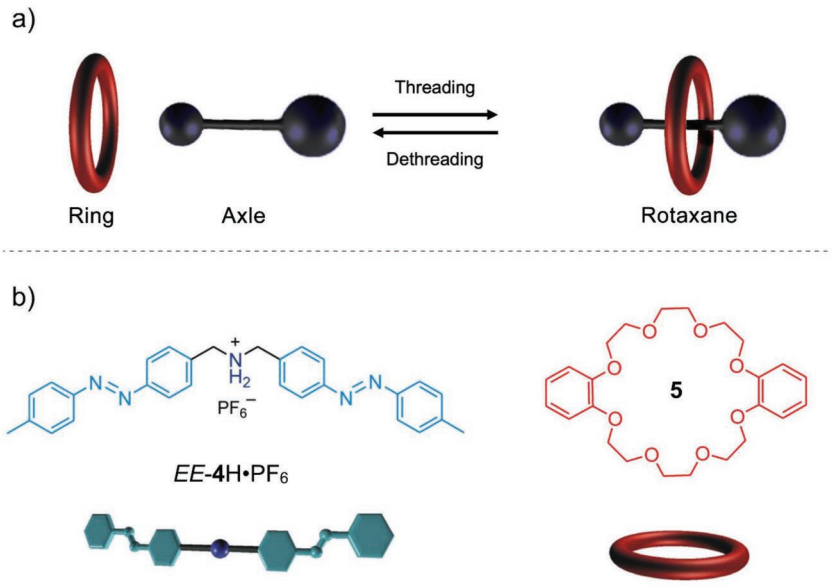

Figure 7. a) Schematic representation of the threading/dethreading movements in a rotaxane-type molecular interlocked system. b) Molecular formula and cartoon representation of the axle and ring components of a photoswitchable rotaxane molecular machine.

cross-disciplinary, encompassing concepts and activities in the fields of chemistry, physics, biology, materials science, engineering, information technology, and medicine. Prospective applications include the use of molecular machines as nanoscale tweezers, valves, motors, switches, memories, logic gates, and catalysts.[52]

The unique dynamic behavior of MIMs—chemical species in which molecular components are held together by mechanical bonds—makes them ideal candidates for the realization of molecular devices and machines.[53] In MIMs, the lack of intercomponent covalent bonds allows for free relative movements of the constituent molecules, while the mechanical bond prevents the complete dissociation of the different parts.

Rotaxanes are a class of MIMs composed of a macrocycle surrounding an axle molecule, as schematically represented in **Figure 7**a. Rotaxanes are usually self-assembled in solution by exploiting the molecular recognition between the ring and axle components arising from non-covalent interactions (for example, hydrogen bonding or electron donor–acceptor interactions).[54] In rotaxanes, the ring is prevented from dethreading from the axle component by the presence of bulky groups at the extremities of the axle—the stoppers. Instead, if the steric hindrance of the end groups is small enough to allow the dethreading of the ring component, under some realistic experimental condition, the term pseudorotaxane is applied to the assembly. Thus, the pseudorotaxane or rotaxane character of a given ring–axle pair is determined by the threading–dethreading rate constants through the end groups of the axle moiety. The kinetic of these processes depends on the temperature and the energy barriers associated with the slipping of the ring on the bulky end groups. Indeed, rotaxanes are topologically equivalent to their non-threaded molecular components, and pseudorotaxanes belong to the fuzzy domain between the two extremes corresponding to the two isolated components and the kinetically interlocked rotaxane structure.[55]

The possibility of modulating the threading–dethreading kinetics of an interlocked ring–axle system by switching the corresponding energy barriers through an external stimulus has interesting implications in terms of controlling the architecture of a supramolecular system and modulating its physico-chemical properties. Moreover, it is a starting point for the construction of rotaxane-like species exhibiting relative unidirectional movements of the components, an important step forward in the development of artificial molecular motors.[13]

By exploiting the large geometrical change associated with azobenzene photoisomerization, we have developed a simple supramolecular system in which the switching between a thermodynamically stable (pseudorotaxane) and kinetically inert (rotaxane) state is controlled by light.[56] The molecular structure of the axle and ring components, respectively *EE*-**4**H•PF_6 and **5**, is shown in Figure 7b. The molecular axle *EE*-**4**H•PF_6 presents a secondary ammonium center and two azobenzene end groups. In solvents of low polarity (e.g., dichloromethane), *EE*-**4**H•PF_6 and the crown ether macrocycle dibenzo-24-crown-8 (**5**) self-assemble into a pseudorotaxane type complex (**Figure 8**, process i→iii), on account of hydrogen bonding between the oxygen atoms of the crown ether and the N^+—H and C—H groups of the secondary ammonium center of the axle. Upon *E*→*Z* photoisomerization of both azobenzene moieties of axle *EE*-**4**H•PF_6, the kinetics of threading–dethreading of ring **5** through *ZZ*-**4**H•PF_6 slows down by four orders of magnitude (Figure 8, process ii→iv).

The sequential behavior of this self-assembling system (i.e., the fact that its behavior depends not only on the type of stimuli but also on their sequence) is evident from the observations shown in **Figure 9**, and results from the possibility of optical switching between a thermodynamically or kinetically controlled self-assembling system.[57] The ^{1}H NMR spectrum shown in Figure 9a was recorded from an equimolar solution of *EE*-**4**H•PF_6 and **5** exhaustively irradiated at 365 nm to cause the *E*→*Z* isomerization of the azobenzene terminal moieties, whose photoreactivity is not affected by the presence of the macrocycle. This spectrum exhibits the characteristic signals indicative of the formation of the [*ZZ*-**4**H•PF_6⊂**5**]$^+$ complex. Conversely, if a solution of *EE*-**4**H•PF_6 is previously exhaustively irradiated at 365 nm and then an equimolar amount of the macrocycle is added, its ^{1}H NMR spectrum presents only signals of the separated molecular components (Figure 9b). This means that no association between the ring and axle takes place on a short time scale because of the very slow threading of *ZZ*-**4**H^+ into **5**.

The interactions that hold the axle threaded through the ring can be cancelled by deprotonation of the ammonium center with a base, that is, using a stimulus orthogonal to that employed for switching the azobenzene end units (Figure 8, processes iii→v and iv→vi). ^{1}H NMR spectroscopy experiments

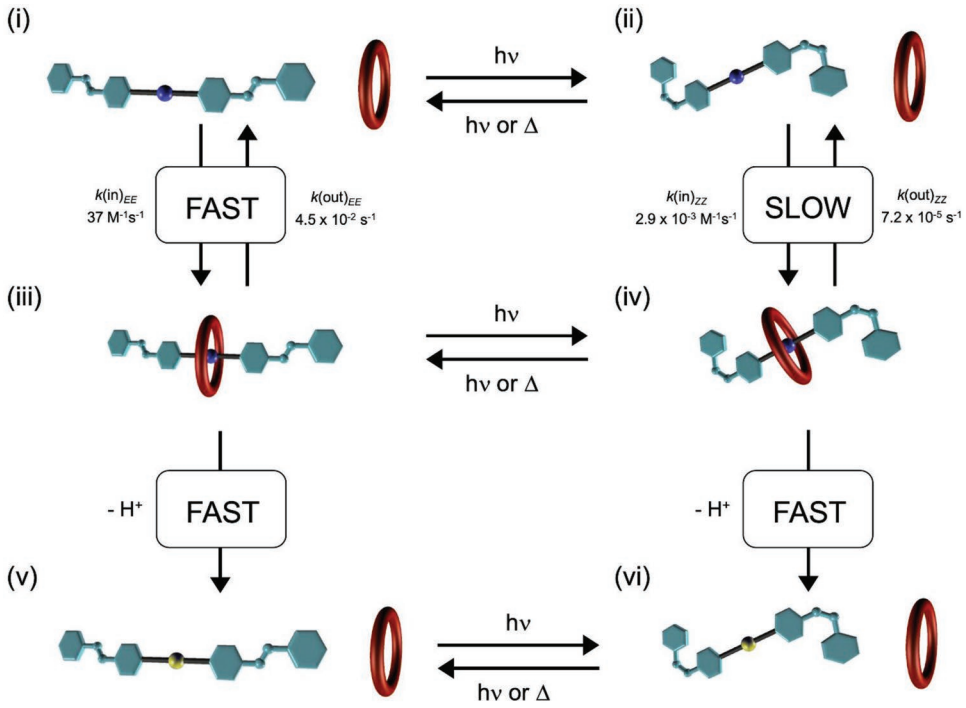

Figure 8. Representation of the self-assembly equilibria and deprotonation reactions (vertical processes) and photoisomerization (horizontal processes) involving the axle and ring components (kinetic constants measured in acetonitrile at 298 K).

demonstrate that deprotonation of the ammonium center of the [*EE*-**4**H⊂**5**]$^+$ complex with a stoichiometric amount of triethylamine (TEA) causes the fast and quantitative dethreading of the pseudorotaxane (Figure 8, process iii→v). Interestingly, the same behavior is observed upon addition of TEA to [*ZZ*-**4**H⊂**5**]$^+$ (Figure 8, process iv→vi) indicating that the barrier to dethreading experienced by the ring is substantially lowered in response to removal of the ammonium recognition motif, irrespective of the isomerization state of the azobenzene end groups. Such an effect is probably a consequence of the proximity of the ammonium recognition site and azobenzene pseudo-stoppers.

This system represents a simple interlocked architecture in which the occurrence and kinetics of the relative motion of the molecular components can be controlled by external chemical and light inputs. The operation of the system is fully reversible and conduces to a marked change in the stoichiometry and chemical and physical properties of the system itself. For these reasons, multi-responsive systems like the one described here are highly promising for the design of tailor-made functional materials. A key issue in this regard is the ability to operate in matrices more complex and organized than liquid solutions.[58]

3.3. Nanofibers Embedding Photo-Controlled Molecular Machines

Until now, most studies on molecular machines have been performed on liquid solutions, as exemplified by the system described in the previous section. Working in solution is convenient under an experimental point of view; moreover, the fluid environment does not put serious constraints on the molecular rearrangements at the base of the machine operation, which in some cases is directly assisted by the solvent molecules. The random distribution of freely diffusing molecules in solution, however, precludes a spatially controlled addressing of individual species or of an ensemble of them in a coherent way, which is a fundamental requisite to turn molecular-scale movements into mesoscopic and macroscopic changes in a material. Therefore, there is a growing interest in making hybrid systems by embedding molecular machines into solid host materials. Various research groups have put effort in the development of viable strategies for introducing functional molecular machines into host matrices, delivering proper stimuli, and detecting the resulting changes. Examples include molecular devices deposited on surfaces,[59] embedded in solid and liquid crystals and gels,[60] linked to nanoparticles,[61] and entrapped into the cavities of metal and covalent organic frameworks.[62]

Relatively few studies deal with polymers as host materials for molecular machines.[63] The plastic properties of polymers can enable the manipulation of the embedded functional moieties, and provide a way to induce a spatial organization of the molecular guests. Moreover, appropriately chosen polymers can assure the transparency to the wavelengths of light needed to switch the state of the incorporated nanomachines, and to sense their state in real time by optical signals. Indeed, azobenzene-based photochromic moieties have been integrated in diverse types of polymeric matrices to achieve photo-controlled reversible morphological changes induced by the isomerization of the azobenzene units.[64] The large variety of polymers with tailored physico-chemical properties, the easy processability, and low cost are further elements that make this type of

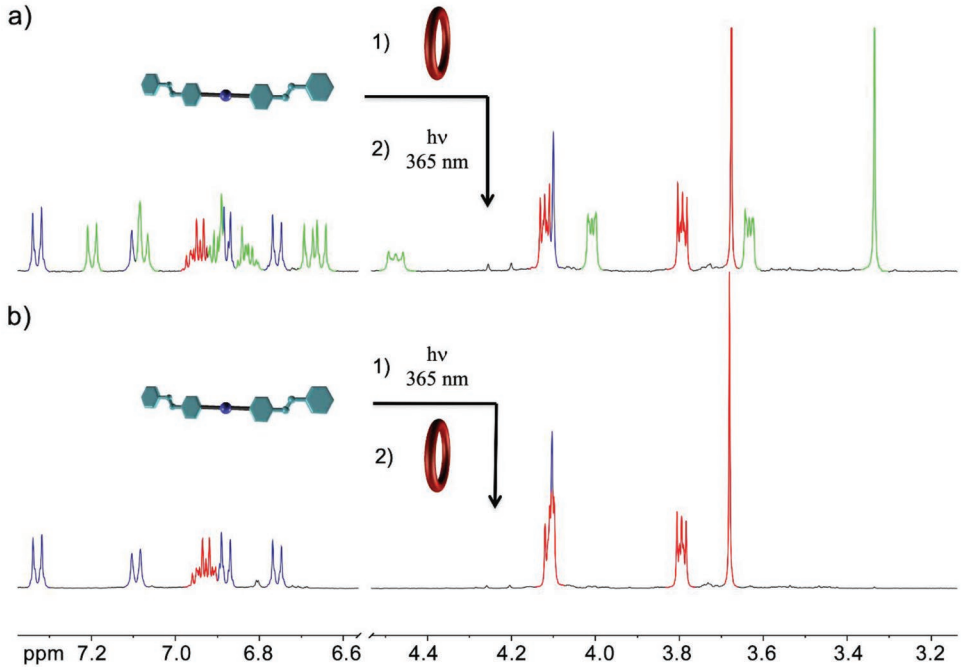

Figure 9. ^{1}H NMR spectra (400 MHz, CD_3CN, 298 K, 3 mM) of *EE*-**4**H$^+$ after a) the addition of one equivalent of **5** followed by exhaustive irradiation at $\lambda = 365$ nm and b) the same inputs in reverse order. The resonances associated with *ZZ*-**4**H$^+$, **5**, and [*ZZ*-**4**H⊂**5**]$^+$ are colored in blue, green, and red, respectively. Adapted with permission.[56] Copyright 2010. Wiley-VCH.

matrices of high interest. Moreover, the nanostructuring of polymers enables a further degree of control on the geometry and morphology of the embedded molecular moieties, affording an increase of the surface-to-volume ratio, and making the interactions with the surrounding matrix more efficient.[65] In particular, polymer nanofibers made by electrospinning exhibit different advantages, such as flexibility, tunability of their composition, morphology and alignment, and ease of integration in optical and electronic devices.[66] Of relevance for the present discussion is the fact that the high stretching rate of the electrified jet at the base of the electrospinning process favors a preferential orientation of both the polymer macromolecules and the embedded dopants.[67]

In order to investigate the combination of these unique properties with the features of artificial molecular machines, we developed electrospun nanocomposites embedding the self-assembling system described in the preceding section that, as illustrated earlier, is responsive to both optical (UV–vis light) and chemical (acid/base) stimuli.[68] Since the solution studies showed that the *E*→*Z* photoisomerization of the terminal azobenzene units converts the supramolecular system between thermodynamically stable (pseudorotaxane) and kinetically inert (rotaxane) forms characterized by markedly different properties, we decided to investigate the effect of this transformation on the properties of nanofiber mats embedding such a prototypical photochemically and chemically addressable supramolecular system.[56]

The threaded complex composed of the axle molecule *EE*-**4**H•PF_6 and ring component **5** (Figure 7b) was embedded in nanofibers made of poly(methyl methacrylate) (PMMA). Due to its excellent plastic behavior, processability, and optical transparency (up to 93% in the visible spectral range), PMMA is an optimal host matrix for photoactive compounds.[69] The nanofibers, which in their pristine form incorporate the self-assembled [*EE*-**4**H•PF_6⊂**5**]•PF_6 pseudorotaxane complex, are amenable to different photochemical and chemical processes, as schematized in **Figure 10**. Light irradiation at 365 nm induces the *E*→*Z* photoisomerization of the azobenzene end groups of the axle moieties embedded into the nanofibers (processes i → ii and iii → iv in Figure 10). The initial state can be restored upon *Z*→*E* conversion of the azobenzene groups by irradiation with 405 nm light or thermal treatment (processes ii → i and iv → iii). Furthermore, on the basis of the solution behavior, deprotonation of the ammonium recognition site with a base is expected to cause the disassembly of the complex, as schematized in processes i → iii and ii → iv in Figure 10. Eventually, treatment with an acid can cause reprotonation of the amine center and trigger the rethreading of the axle component through the crown ether ring (processes iii → i and iv → ii).

The possibility to address the state of the nanomachines by orthogonal light and chemical inputs combined with the weak nonbonding interactions between the components of the nanomachines themselves and the surrounding polymeric matrix can indeed yield a responsive material sensible to external stimuli of different nature. The dethreading and rethreading of the axle and ring components in the fibers, induced by exposure to base and acid vapors, respectively, further endow this hybrid composite architecture with the potential for application as a chemical sensor.

The occurrence of *E*→*Z* photoisomerization of the pseudorotaxane complexes induced by irradiation with UV laser light

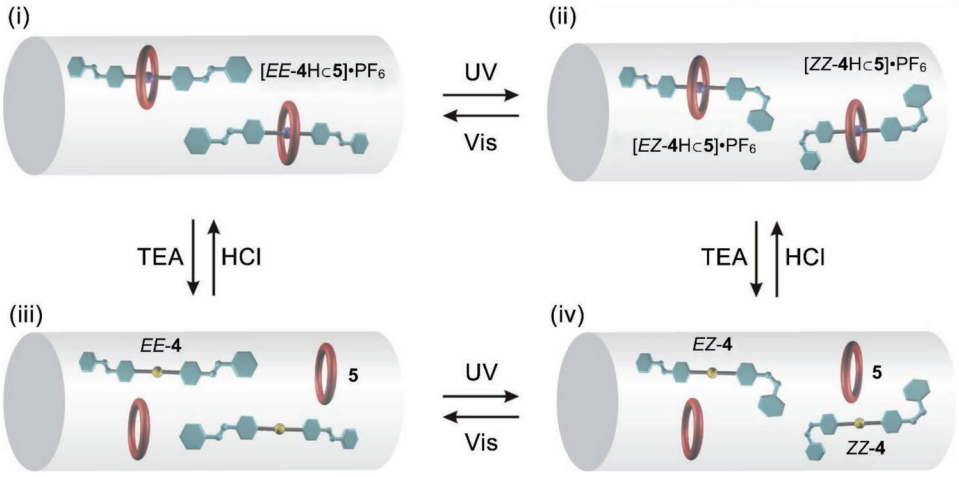

Figure 10. Schematic representation of the *E*-*Z* photoisomerization of the azobenzene end groups of the axle and chemical deprotonation/protonation-induced dethreading/rethreading processes that the axle and ring molecular components can undergo inside the nanofibers. Adapted with permission.[68] Copyright 2014, American Chemical Society.

(process i → ii in Figure 10) incorporated into the nanofibers was assessed by analyzing the characteristic changes in the UV–vis absorption spectrum (**Figure 11**a). The intensity of the peak at 325 nm, characteristic of the *EE*-form of the axle moiety, decreases with increasing UV exposure time, as shown in Figure 11b. A photostationary state is reached upon irradiation for about 20 min, after which no more changes in the absorption intensity are observed. Based on the solution absorption spectra of *EE*-**4**H•PF_6 and *ZZ*-**4**H•PF_6, the absorbance of the *Z*-azobenzene unit at 325 nm is negligible compared to that of the *E*-isomer. Hence, the absorption changes demonstrate that about 40% of the *E*-azobenzene units present in nanofibers are transformed to the *Z*-form upon UV light irradiation.

Exposure of the UV-irradiated samples to 405 nm light induces opposite spectral changes (Figure 11c), indicative of the back conversion of the *Z*-azobenzene units to the *E* form (process ii → i in Figure 10). The initial value of absorption intensity at 325 nm is completely recovered after about 10 min of irradiation (Figure 11d), indicative of a quantitative photoisomerization of the axle molecules back to the original *EE*-form. This result demonstrates both the reversibility of azobenzene photoisomerization in the polymer environment and, more interestingly, the excellent photochemical properties of the axle which are retained in nanofibers. The photoinduced switching of the azobenzene moieties is highly efficient and reversible, as shown by consecutive cycles of alternated irradiation with UV and blue light, evidencing the fatigue resistance of the system (Figure 11e).

During the electrospinning process the stretching of the polymeric fibers induced by the applied electric field allows a partial control on the prevalent orientation of the polymeric chains and, as a consequence, also of the embedded molecular components of the nanomachines. Indeed, polarized infrared spectroscopy measurements confirmed a partial alignment of the PMMA polymeric chains and of the [*EE*-**4**H⊂**5**]·PF_6 complex along the main axis of the nanofibers, induced by the electrospinning process.

Upon switching on and off the recognition site on the axle by protonation and deprotonation of the ammonium moiety, one may expect to induce the dethreading and rethreading motion of the ring–axle system embedded in the fibers, in line with the solution behavior. To this aim, electrospun samples incorporating [*EE*-**4**H⊂**5**]·PF_6 were exposed alternatively to basic (TEA) and acid (HCl) vapors, and the resulting samples were analyzed by fluorescence spectroscopy. In solution, the ring has a characteristic fluorescence emission with a maximum at 310 nm, whose intensity decays to zero upon association with a molecular axle containing the azobenzene units in either the *E* or *Z* configuration.[70] Since the luminescence features of the axle and the ring are preserved upon electrospinning the molecular components with PMMA, the measurements of the fluorescence of the nanofibers provide a simple mean to evaluate whether the axle and ring components are associated or not. The intensity of the emission band at 310 nm (**Figure 12**a), attributed to the free ring molecules embedded into the nanofibers, increases remarkably after exposure to basic TEA vapors (Figure 12b) and decreases again to smaller values after subsequent exposure to acidic HCl vapors (Figure 12c). These results are consistent with a dethreading of the ring from the axle upon deprotonation of the ammonium site, induced by the TEA vapors (Figure 10, process i → iii), and with successive rethreading caused by treatment with acidic vapors (Figure 10, process iii → i). The observed large increase of the fluorescence intensity of the free ring upon exposure to TEA vapors is indicative that the dethreading of the ring is practically quantitative. Moreover, the weak fluorescence observed before exposure to the TEA vapors is almost completely recovered after treatment with HCl vapors (Figure 12a–c). These observations prove that the chemical stimulus represented by TEA vapors is able to cause the disassembly of the threaded complex, which is reversibly reassembled by treatment with HCl, and that the threading–dethreading motion is not hindered by the PMMA chains of the nanofibers.

The dethreading/rethreading kinetics in the nanofibers incorporating the [*EE*-**4**H⊂**5**]·PF_6 complex was investigated by

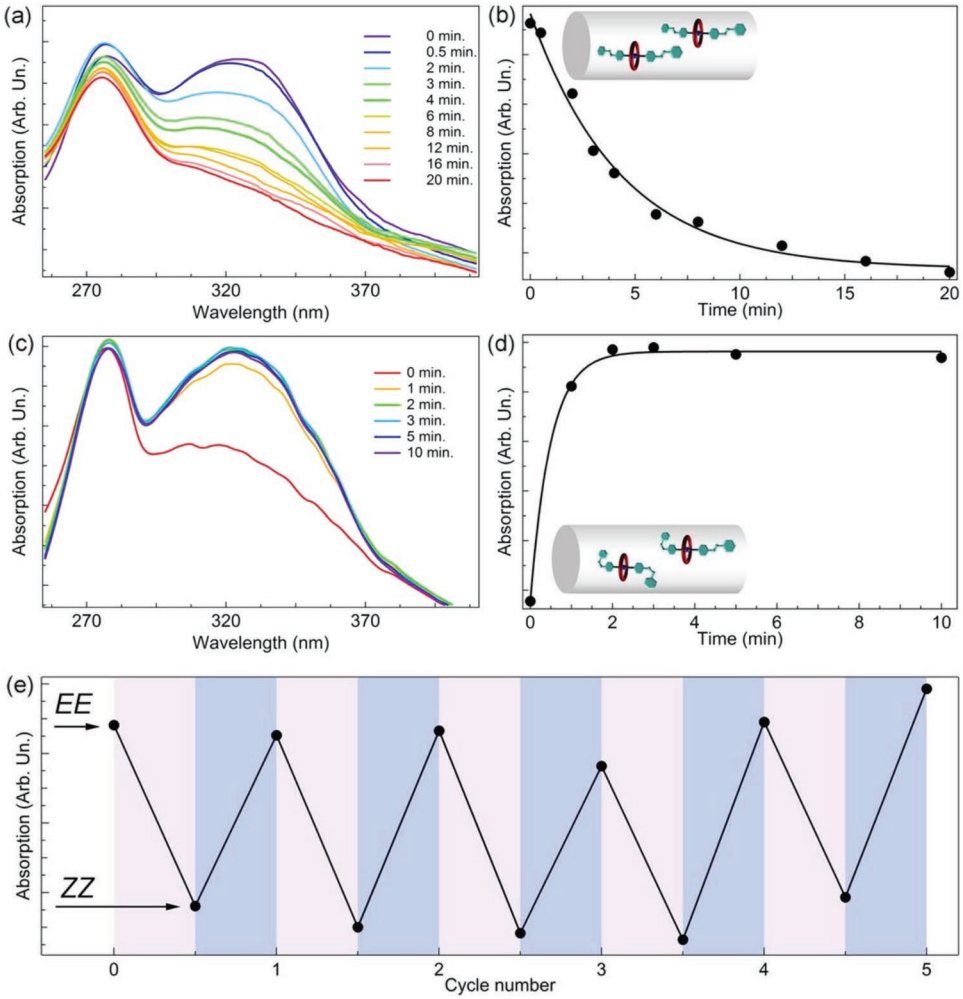

Figure 11. a) Absorption spectra of nanofibers embedding [*EE*-**4**H⊂**5**]·PF_6 upon increasing exposure to 355 nm light. b) Plot of the absorbance changes at 325 nm versus the exposure time of spectra shown in (a); the continuous line is a guide for the eye. c) Absorption spectra of fibers, previously subjected to exhaustive UV irradiation, upon increasing exposure to 405 nm light. d) Plot of the absorbance changes at 325 nm versus the exposure time of spectra shown in (c); the continuous line is a guide for the eye. e) Absorption changes at 325 nm, for consecutive cycles of alternated 355 and 405 nm light irradiation. Reproduced with permission.[68] Copyright 2014, American Chemical Society.

exposing samples of the nanofibers to TEA vapors and, successively, to HCl vapors for variable exposure times in a range between 15 min and 4 h. The observation that the dethreading/rethreading process, as followed by fluorescence spectroscopy, is completed within about 120 min can be attributed to the barrier associated with the molecular movements in the polymer matrix, combined with the dynamics of gas diffusion in electrospun fibers, which is known to occur on a time scale of a few tens of minutes.[71] Furthermore, [*EE*-**4**H⊂**5**]·PF_6 fibers exposed first to UV laser light and then to TEA/HCl do not show significant differences compared to samples directly treated with TEA/HCl, indicating that the dethreading/rethreading (processes ii → iv and iv → ii in Figure 10) of the ring and axle components in the fibers can occur even after the photo-isomerization of the azobenzene units of the axle. Similarly, the *E* →*Z* photoisomerization of the azobenzene units of the axle in the fibers is not significantly affected by the TEA-induced dethreading (processes iii → iv and iv → iii in Figure 10).

The modification of the macroscopic mechanical properties of the nanofibers in response to the switching, upon light and chemical stimulation, of the association state of the integrated ring and axle components is a key objective of this study. The mechanical properties of pristine PMMA nanofibers (i.e., devoid of the molecular machine components) agree with those reported in literature.[72] Indeed, the presence and, more interestingly, the threading and dethreading of the axle and ring components markedly alter the mechanical properties of nanofibers. In particular, while the ultimate tensile strength (**Figure 13**b) and maximum strain (Figure 13c) show negligible changes, large differences are observed for the Young's modulus upon switching the state of the embedded molecular machines. The average Young's modulus of pristine aligned PMMA nanofibers is around (50 ± 10) MPa (a value that is not influenced by exposure of the nanofibers to TEA), and the incorporation of the threaded complex [*EE*-**4**H⊂**5**]·PF_6 doubles this figure (Figure 13a). The Young's modulus of [*EE*-**4**H⊂**5**]·PF_6-doped nanofibers, after exposure to TEA vapors, increases up to

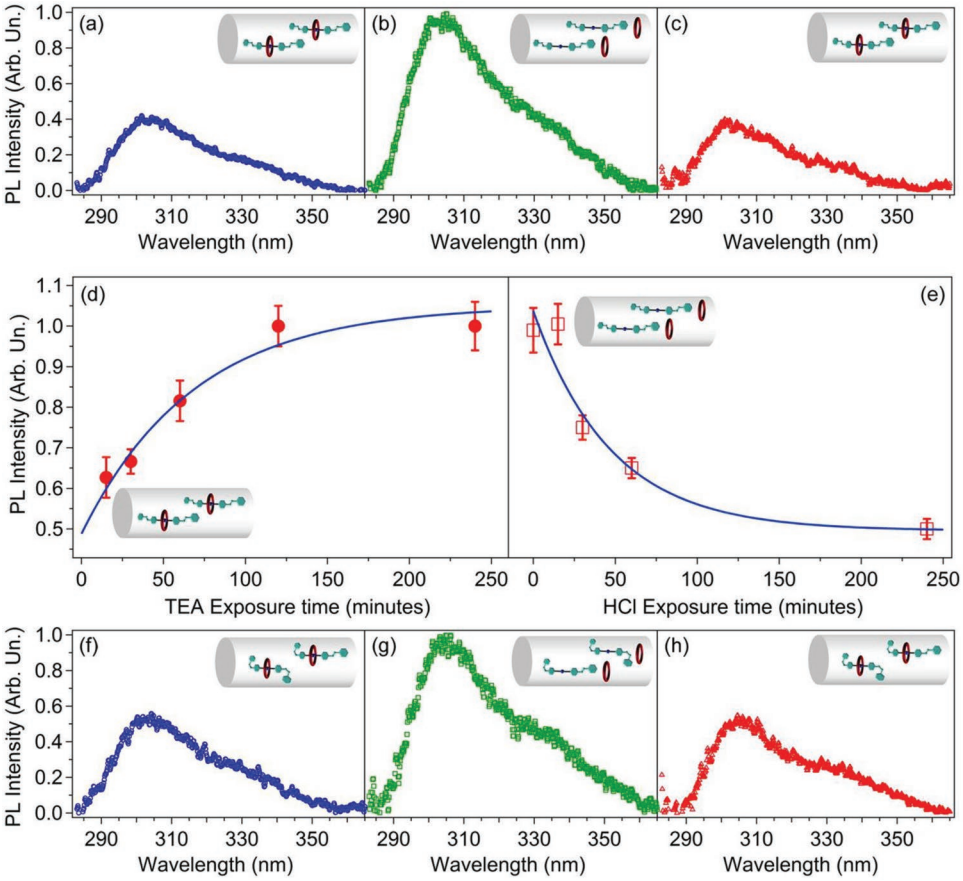

Figure 12. a–c) Fluorescence spectra of nanofibers embedding [*EE*-**4**H⊂**5**]·PF_6, before (a) and after (b) exposure to TEA vapors for 4 h; c) Spectra of the samples shown in (a) and (b) after exposure to HCl vapors for 4 h. d,e) Fluorescence intensity of [*EE*-**4**H⊂**5**]·PF_6-based fibers versus TEA (d) and HCl (e) exposure times. The samples in (e) were first exposed to TEA vapors for 4 h. Continuous lines are guides for the eye. f–h) Fluorescence spectra of [*ZZ*-**4**H⊂**5**]·PF_6-based fibers PMMA, before (f) and after exposure to TEA (g) and HCl (h) vapors, respectively. In all cases, excitation was performed at 266 nm. Reproduced with permission.[68] Copyright 2014, American Chemical Society.

(160 ± 20) MPa, indicative of a considerable increase of the stiffness of the nanofibrous mat upon dethreading of the ring and axle components (Figure 13a). Control experiments carried out on nanofibers doped with the axle molecules only do not present an increase of the Young's modulus, proving that the sole deprotonation of the axle has no influence on the mechanical properties of the nanofibers.

The photoisomerization of the azobenzene end groups by exposure to UV light does not significantly alter the mechanical properties of the fibers. Indeed, the tensile strength and the Young's modulus of [*EE*-**4**H⊂**5**]·PF_6-doped nanofibers (both taken in their pristine state and following TEA treatment) remain almost unaltered after UV irradiation. The above described differences in the mechanical properties when molecular machines are embedded in the fibers can be rationalized considering that both the axle component and the resulting threaded species are considerably more rigid than the PMMA molecules. It may therefore be argued that fibers in which these dopants are partially aligned with the host polymer chains could exhibit an increased stiffness. Following TEA treatment and ring–axle dethreading, the corresponding stress–strain curve becomes sublinear (upward triangles in Figure 13d), suggesting that the fibers undergo a microscopic structural rearrangement conducive to a plastic flow in their strain-hardening regime. This is especially interesting because the Young's modulus of (160 ± 20) MPa reached after dethreading of the ring from the axle is significantly higher than the value found for fibers embedding only the free axle of (100 ± 10) MPa. Taken together, these results indicate that a specific increase of stiffness is associated with fibers embedding dethreaded molecular components. In general, the improvement of mechanical properties in nanocomposites depends on the load transfer to rigid fillers from the plastic matrix. Various mechanisms can improve load transfer, such as micro-mechanical interlocking between the matrix material and the fillers, chemical bonding, or van der Waals interactions. In the present case, dethreaded species can promote load transfer from the plastic matrix due to van der Waals interactions, and correspondingly increase interfacial interactions between the polymer phase.[73] Another effect to be considered is the increase of the number of embedded molecular components in the composite, arising from the separation of the axles from the rings upon dethreading. The observation of a sizeable change on the mechanical properties of polymer nanofibers in response to a change in the ring–axle supramolecular arrangement is a significant step forward toward the exploitation of controlled nanoscale molecular movements

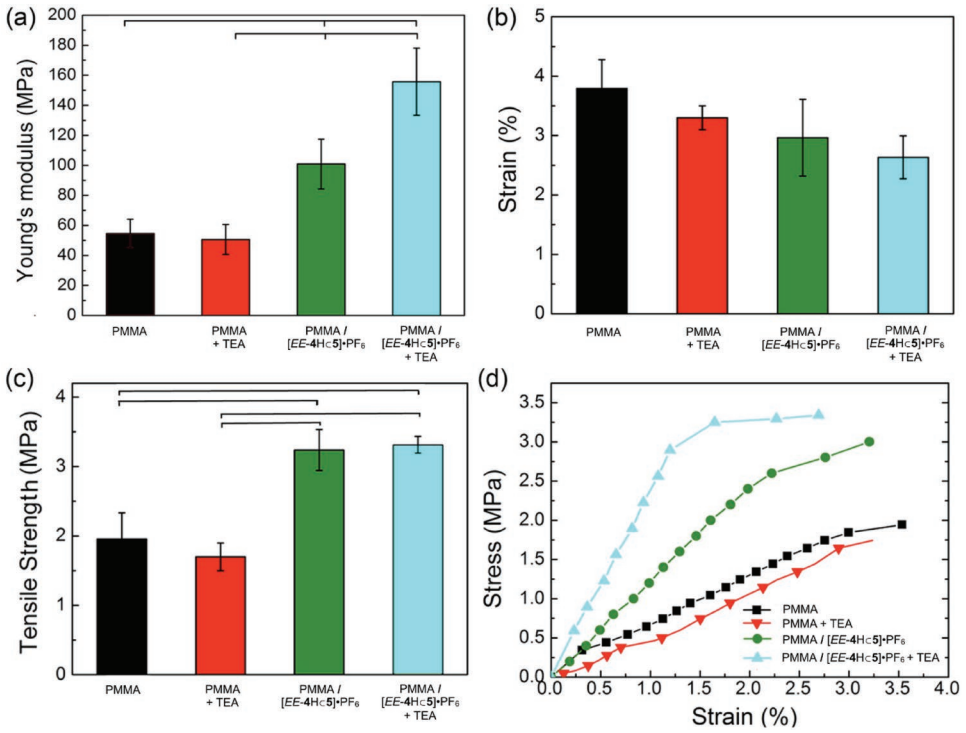

Figure 13. Mechanical properties of PMMA and PMMA/[*EE*-**1**H⊂**2**]·PF_6 nanofibers before and after exposure to TEA vapors: a) Young's modulus, b) strain, and c) tensile strength. The results are expressed as (mean value ± standard deviation). Bars show statistically significant differences ($p < 0.05$). d) Representative stress/strain curves. Reproduced with permission.[68] Copyright 2014, American Chemical Society.

to bring about effects at the macroscopic level. This is a relevant example of a system able to overcome the dimensional gap between the nano- and macro-scale, a problem that is of the highest importance for the real-world application of molecular devices and machines. Moreover, multi-responsive hybrid nanocomposites of this kind are appealing for the development of innovative devices and materials for photonics, (bio)chemical sensing, and molecular release.

4. Conclusion

The studies described in this progress report prove that innovative and fascinating molecular-scale devices and machines capable of performing non-trivial functions can be tailor-made by applying rational design strategies based on the tools of modern synthetic chemistry and the paradigms of supramolecular chemistry. Specifically, the marriage of photochemistry with supramolecular chemistry enables the construction of molecular and supramolecular systems containing photoreactive moieties that can activate and control advanced operations via light stimuli. This goal is achieved by virtue of the drastic photoinduced changes in the physical and chemical properties of suitably chosen building blocks. Azobenzene and its derivatives, owing to their facile synthesis and functionalization complemented by their predictable and highly tuneable photophysical characteristics, are most versatile moieties for implementing light-responsive properties with chemical systems. The systematic search for azobenzene-type photoswitches with improved behavior, as well as the development of novel classes of photochromic species, is surely an important and ever-expanding area of research that can have a strong impact in this context. Materials containing photoswitchable molecular components can be engineered to display drastic changes in fundamental properties such as density, viscosity, electrical conductivity, stiffness, and porosity with a high spatial and temporal resolution.

The coupling of photoswitchable moieties and self-assembly processes in molecular devices and machines represent an innovative and, in our opinion, general approach to endow materials with photoactivatable functionalities without the stringent requirements of direct chemical functionalization. Considering the large number of molecular and supramolecular switching systems and the wide variety of possible host materials, the possibilities are virtually unlimited. At present, the main challenge is to identify viable compromises between the chemical characteristics, operation mechanism and input/output modes of the molecular devices, and the physico-chemical properties, preparation routes, and processing requirements of the matrix, such that the function of the nanodevices is preserved in the hybrid material. An improved understanding of these aspects is expected to provide useful feedbacks for the development of new generations of functional molecular and supramolecular systems designed to work in complex matrices. At some point, real-world applications in fields such as materials engineering, information processing, robotics, and medicine will urge researchers to deal with issues such as energy efficiency, production cost, and effects on health and the environment. Apart from more or less futuristic applications, the rational design and construction of functional nanostructured systems and

materials has the merit of bringing scientists from different disciplines to cooperate and develop a common language.

Acknowledgements

The authors are grateful to all their past and present group members. Fruitful collaboration with professors Angiolina Comotti and Piero Sozzani (Università di Milano-Bicocca), Fabrizia Grepioni (Università di Bologna), Andrea Camposeo (Consiglio Nazionale delle Ricerche), and Dario Pisignano (Università di Pisa) is gratefully acknowledged. This work was supported by the European Union's Horizon 2020 research and innovation program (ERC Advanced Grant "Leaps" no. 692981 and FET-OPEN "Magnify" no. 801378) and the Ministero dell'Istruzione, Università e Ricerca (FARE Grant "Ampli" no. R16S9XXKX3).

Conflict of Interest

The authors declare no conflict of interest.

Keywords

azobenzene photochromes, light actuators, light-responsive chemical systems, molecular architectures, molecular machines, photochromic compounds, photoswitchable molecular materials

Received: March 4, 2019
Revised: April 15, 2019
Published online:

[1] *Photobiology: The Science of Life and Light* (Ed: L. O. Björn), Springer, New York, **2008**.
[2] C. Yeh, *Applied Photonics*, Academic Press, Elsevier, San Diego, CA **1994**.
[3] J. M. Lehn, *Angew. Chem. Int. Ed.* **1988**, *27*, 89.
[4] K. C. Nicolaou, *Isr. J. Chem.* **2018**, *58*, 104.
[5] *Supramolecular Chemistry* (Eds: P. A. Gale, J. W. Steed), John Wiley & Sons, Chichester, UK **2012**.
[6] C. J. Bruns, J. F. Stoddart, *The Nature of the Mechanical Bond*, John Wiley & Sons, Hoboken, NJ **2016**.
[7] V. Balzani, A. Credi, M. Venturi, *Chem. - Eur. J.* **2002**, *8*, 5524.
[8] V. Balzani, A. Credi, M. Venturi, *Molecular Devices and Machines: Concepts and Perspectives for the Nanoworld: Second Edition*, Wiley-VCH Verlag, Weinheim **2008**.
[9] E. R. Kay, D. A. Leigh, F. Zerbetto, *Angew. Chem. Int. Ed.* **2007**, *46*, 72.
[10] a) J.-P. Sauvage, *Angew. Chem. Int. Ed.* **2017**, *56*, 11080; b) J. F. Stoddart, *Angew. Chem. Int. Ed.* **2017**, *56*, 11094; c) B. L. Feringa, *Angew. Chem. Int. Ed.* **2017**, *56*, 11060.
[11] S. Mann, *Angew. Chem. Int. Ed.* **2008**, *47*, 5306.
[12] a) C. Cheng, J. F. Stoddart, *Chem Phys Chem* **2016**, *17*, 1780; b) T. Muraoka, K. Kinbara, *J. Photochem. Photobiol. C* **2012**, *13*, 136.
[13] M. Baroncini, L. Casimiro, C. de Vet, J. Groppi, S. Silvi, A. Credi, *Chemistry Open* **2018**, *7*, 169.
[14] P. Ceroni, A. Credi, M. Venturi, *Chem. Soc. Rev.* **2014**, *43*, 4068.
[15] L. Wang, Q. Li, *Chem. Soc. Rev.* **2018**, *47*, 1044.
[16] a) O. S. Bushuyev, C. J. Barrett, *Photochromism in the Solid State*, John Wiley & Sons, Chichester, UK **2017**; b) *Photochromic Materials: Preparation, Properties and Applications* (Eds: H. Tian, J. Zhang), Wiley-VCH Verlag, Weinheim **2016**.
[17] D. Bléger, S. Hecht, *Angew. Chem. Int. Ed.* **2015**, *54*, 11338.
[18] J. Griffiths, *Chem. Soc. Rev.* **1972**, *1*, 481.
[19] V. Balzani, P. Ceroni, A. Juris, *Photochemistry and Photophysics: Concepts, Research, Applications*, Wiley-VCH Verlag, Weinheim **2014**.
[20] H. Dürr, H. Bouas-Laurent, *Photochromism: Molecules and Systems*, Elsevier, Amsterdam **2003**.
[21] E. Mitscherlich, *Eur. J. Org. Chem.* **1834**, *12*, 311.
[22] A. Noble, *Eur. J. Org. Chem.* **1856**, *98*, 253.
[23] C. V. Gortner, R. A. Gortner, *J. Am. Chem. Soc.* **1910**, *32*, 1294.
[24] G. S. Hartley, *J. Chem. Soc.* **1938**, *0*, 633.
[25] M. Baroncini, G. Ragazzon, S. Silvi, M. Venturi, A. Credi, *Pure Appl. Chem.* **2015**, *87*, 537.
[26] K. Ichimura, *Chem. Rev.* **2000**, *100*, 1847.
[27] Z. Mahimwalla, K. G. Yager, J.-I. Mamiya, A. Shishido, A. Priimagi, C. J. Barrett, *Chem. Heterocycl. Compd.* **2012**, *69*, 967.
[28] M. Zhu, H. Zhou, *Org. Biomol. Chem.* **2018**, *16*, 8434.
[29] a) Y. Hao, S. Huang, Y. Guo, L. Zhou, H. Hao, C. J. Barrett, H. Yu, *J. Mater. Chem. C* **2019**, *47*, 1044; b) M. Yamada, M. Kondo, J.-I. Mamiya, Y. Yu, M. Kinoshita, C. J. Barrett, T. Ikeda, *Angew. Chem. Int. Ed.* **2008**, *47*, 4986; c) H. Yu, T. Kobayashi, *Molecules* **2010**, *15*, 570.
[30] L. Dong, Y. Feng, L. Wang, W. Feng, *Chem. Soc. Rev.* **2018**, *46*, 52.
[31] a) E. Merino, *Chem. Soc. Rev.* **2011**, *40*, 3835; b) C. Knie, M. Utecht, F. Zhao, H. Kulla, S. Kovalenko, A. M. Brouwer, P. Saalfrank, S. Hecht, D. Bléger, *Chem. - Eur. J.* **2014**, *20*, 16492.
[32] M. Ishikawa, T. Ohzono, T. Yamaguchi, Y. Norikane, *Sci. Rep.* **2017**, *7*, 6909.
[33] Ľ. Vetráková, V. Ladányi, J. Al Anshori, P. Dvořák, J. Wirz, D. Heger, *Photochem. Photobiol. Sci.* **2017**, *16*, 1749.
[34] H. Rau, *Photochemistry and Photophysics* (Ed: J. F. Rabek), CRC Press, Boca Raton, FL **1990**, p. 119.
[35] T. Schultz, J. Quenneville, B. Levine, A. Toniolo, T. J. Martínez, S. Lochbrunner, M. Schmitt, J. P. Shaffer, M. Z. Zgierski, A. Stolow, *J. Am. Chem. Soc.* **2003**, *125*, 8098.
[36] C. J. Otolski, A. Mohan Raj, V. Ramamurthy, C. G. Elles, *J. Phys. Chem. Lett.* **2018**, *10*, 121.
[37] A. Cembran, F. Bernardi, M. Garavelli, L. Gagliardi, G. Orlandi, *J. Am. Chem. Soc.* **2004**, *126*, 3234.
[38] H. M. D. Bandara, S. C. Burdette, *Chem. Soc. Rev.* **2012**, *41*, 1809.
[39] K. Stranius, K. Börjesson, *Sci. Rep.* **2017**, *7*, 41145.
[40] J. Zhang, H. Tian, *Adv. Opt. Mater.* **2018**, *6*, 1701278.
[41] M. Irie, T. Fukaminato, K. Matsuda, S. Kobatake, *Chem. Rev.* **2014**, *114*, 12174.
[42] a) O. S. Bushuyev, T. Friščič, C. J. Barrett, *CrystEngComm* **2016**, *38*, 7204; b) R. D. Mukhopadhyay, V. K. Praveen, A. Ajayaghosh, *Mater. Horiz.* **2014**, *1*, 572.
[43] M. Baroncini, S. d'Agostino, G. Bergamini, P. Ceroni, A. Comotti, P. Sozzani, I. Bassanetti, F. Grepioni, T. M. Hernandez, S. Silvi, M. Venturi, A. Credi, *Nat. Chem.* **2015**, *7*, 634.
[44] W. Guo, E. Galoppini, R. Gilardi, G. I. Rydja, Y.-H. Chen, *Cryst. Growth Des.* **2001**, *1*, 231.
[45] I. Aujard, J. P. Baltaze, J. B. Baudin, E. Cogné, F. Ferrage, L. Jullien, E. Perez, V. Prévost, L. M. Qian, O. Ruel, *J. Am. Chem. Soc.* **2001**, *123*, 8177.
[46] J. R. Holst, A. Trewin, A. I. Cooper, *Nat. Chem.* **2010**, *2*, 915.
[47] K. H. Bennemann, *J. Phys. Condens. Matter.* **2011**, *23*, 073202.
[48] a) H. Akiyama, S. Kanazawa, Y. Okuyama, M. Yoshida, H. Kihara, H. Nagai, Y. Norikane, R. Azumi, *ACS Appl. Mater. Interfaces* **2014**, *6*, 7933; b) Y. Norikane, E. Uchida, S. Tanaka, K. Fujiwara, E. Koyama, R. Azumi, H. Akiyama, H. Kihara, M. Yoshida, *Org. Lett.* **2014**, *16*, 5012.
[49] a) Y. Kobayashi, J. Abe, *Adv. Opt. Mat.* **2016**, *4*, 1354; b) U. Pischel, J. Andréasson, D. Gust, V. F. Pais, *ChemPhysChem* **2013**, *14*, 28.
[50] C. Nacci, M. Baroncini, A. Credi, L. Grill, *Angew. Chem. Int. Ed.* **2018**, *57*, 15034.

[51] T. Bura, M. P. Gullo, B. Ventura, A. Barbieri, R. Ziessel, *Inorg. Chem.* **2013**, *52*, 8653.
[52] A. Coskun, M. Banaszak, R. D. Astumian, J. F. Stoddart, B. A. Grzybowski, *Chem. Soc. Rev.* **2011**, *41*, 19.
[53] J. P. Sauvage, C. Dietrich-Buchecker, *Molecular Catenanes, Rotaxanes and Knots*, Wiley-VCH Verlag, Weinheim **1999**.
[54] P. R. Ashton, P. J. Campbell, P. T. Glink, D. Philp, N. Spencer, J. F. Stoddart, E. J. T. Chrystal, S. Menzer, D. J. Williams, P. A. Tasker, *Angew. Chem. Int. Ed.* **1995**, *34*, 1865.
[55] P. R. Ashton, I. Baxter, M. C. T. Fyfe, F. M. Raymo, N. Spencer, J. F. Stoddart, A. J. P. White, D. J. Williams, *J. Am. Chem. Soc.* **1998**, *120*, 2297.
[56] M. Baroncini, S. Silvi, M. Venturi, A. Credi, *Chem. - Eur. J.* **2010**, *16*, 11580.
[57] T. Avellini, M. Baroncini, G. Ragazzon, S. Silvi, M. Venturi, A. Credi, *Isr. J. Chem.* **2014**, *54*, 553.
[58] V. Balzani, A. Credi, M. Venturi, *ChemPhysChem* **2008**, *9*, 202.
[59] a) E. Coronado, P. Gaviña, S. Tatay, *Chem. Soc. Rev.* **2009**, *38*, 1674; b) Q. Zhang, D.-H. Qu, *ChemPhysChem* **2016**, *17*, 1759.
[60] C. S. Vogelsberg, M. A. Garcia-Garibay, *Chem. Soc. Rev.* **2012**, *41*, 1892.
[61] S. Angelos, E. Johansson, J. F. Stoddart, J. I. Zink, *Adv. Func. Mat.* **2007**, *17*, 2261.
[62] V. N. Vukotic, K. J. Harris, K. Zhu, R. W. Schurko, S. J. Loeb, *Nat. Chem.* **2012**, *4*, 456.
[63] a) D. A. Leigh, M. A. F. Morales, E. M. Pérez, J. K. Y. Wong, C. G. Saiz, A. M. Z. Slawin, A. J. Carmichael, D. M. Haddleton, A. M. Brouwer, W. J. Buma, G. W. H. Wurpel, S. León, F. Zerbetto, *Angew. Chem. Int. Ed.* **2005**, *44*, 3062; b) T. Uyar, P. Kingshott, F. Besenbacher, *Angew. Chem. Int. Ed.* **2008**, *47*, 9108.
[64] A. Natansohn, P. Rochon, *Chem. Rev.* **2002**, *102*, 4139.
[65] a) K. Ariga, H. Ito, J. P. Hill, H. Tsukube, *Chem. Soc. Rev.* **2012**, *41*, 5800; b) N. Hosono, T. Kajitani, T. Fukushima, K. Ito, S. Sasaki, M. Takata, T. Aida, *Science* **2010**, *330*, 808.
[66] D. Li, Y. Xia, *Adv. Mater.* **2004**, *16*, 1151.
[67] X. Lu, C. Wang, Y. Wei, *Small* **2009**, *5*, 2349.
[68] V. Fasano, M. Baroncini, M. Moffa, D. Iandolo, A. Camposeo, A. Credi, D. Pisignano, *J. Am. Chem. Soc.* **2014**, *136*, 14245.
[69] F. Di Benedetto, E. Mele, A. Camposeo, A. Athanassiou, R. Cingolani, D. Pisignano, *Adv. Mater.* **2008**, *20*, 314.
[70] G. Rogez, B. F. Ribera, A. Credi, R. Ballardini, M. T. Gandolfi, V. Balzani, Y. Liu, B. H. Northrop, J. F. Stoddart, *J. Am. Chem. Soc.* **2007**, *129*, 4633.
[71] A. Camposeo, F. Di Benedetto, R. Stabile, R. Cingolani, D. Pisignano, *App. Phys. Lett.* **2007**, *90*, 143115.
[72] C. S. Reddy, A. Zak, E. Zussman, *J. Mater. Chem.* **2011**, *21*, 16086.
[73] L. S. Schadler, S. C. Giannaris, P. M. Ajayan, *App. Phys. Lett.* **1998**, *73*, 3842.

